Application of ultrasound to noninvasive imaging of temperature distribution induced in tissue

Piotr KARWAT, Tamara KUJAWSKA, Wojciech SECOMSKI, Barbara GAMBIN, Jerzy LITNIEWSKI

Institute of Fundamental Technological Research, Polish Academy of Sciences, Pawińskiego 5B,Warsaw, Poland
jlitn@ippt.pan.pl

Therapeutic and surgical applications of High Intensity Focused Ultrasound (HIFU) require monitoring of local temperature rises induced inside tissues. It is needed to appropriately target the focal plane, and hence the whole focal volume inside the tumor tissue, prior to thermo-ablative treatment, and the beginning of tissue necrosis. In this study we present an ultrasound method, which calculates the variations of the speed of sound in the locally heated tissue. Changes in velocity correspond to temperature change. The method calculates a 2D distribution of changes in the sound velocity, by estimation of the local phase shifts of RF echo-signals backscattered from the heated tissue volume (the focal volume of the HIFU beam), and received by an ultrasound scanner (23). The technique enabled temperature imaging of the heated tissue volume from the very inception of heating. The results indicated that the contrast sensitivity for imaging of relative changes in the sound speed was on the order of 0.06%; corresponding to an increase in the tissue temperature by about 2 °C.

Keywords: HIFU, echo phase shift, parametric imaging, velocity/brightness CNR

1. Introduction

Besides the well-known ultrasonic diagnostic applications of ultrasound, ultrasonic waves are increasingly used in therapeutic treatments (active ultrasound). Here, one can distinguish, the quickly-developing medical technique of HIFU (High Intensity Focused Ultrasound), which involves the destruction of cancer cells by heating them using a highly focused beam of ultrasound. Studies are also underway on the heating of tissues to temperatures below the denaturation of proteins (hyperthermia). In this case, the treatment involves inducing heat shock, which results in increased enhanced production of HSP proteins (Heat Shock Protein). These proteins, known as chaperones, acting on the protein chains, unfolded by heat, restore their proper conformation and, during this process, at the same time,

repair other damaged structures. Often the treatment of hyperthermia is used in combination with radiation therapy and chemotherapy. Increase of temperature of the tissue causes the tumor to be more sensitive to radiotherapy / chemotherapy treatment. The main problem is to estimate the temperature in the treatment area. Exact knowledge of the temperature distribution in the region of therapy, and its changes during heating, undoubtedly increases the efficiency, and reduces the risk, of treatment. All thermal therapy treatments require the monitoring of the heating of the tissue. The final aim of the research was to develop an ultrasonic method for the preparation of maps; maps of the temperature distribution induced locally inside the tissue and its evolution over time. The method should operate effectively, in particular, in the temperature range below the threshold for thermal damage (1) in soft tissue.

Heating process can be monitored using magnetic resonance imaging techniques (MRI) (2). These techniques, however, have several disadvantages. It is difficult to carry out in real-time monitoring of the therapy using MR systems; due to the slow process of image acquisition. Additionally, it is very expensive, and requires a maximum reduction of metal parts. These restrictions are the cause of the very slow development of MR-assisted HIFU therapy. The use of ultrasonic imaging methods carries a number of advantages relevant to the imaging process of thermal treatment. In this case, imaging can be performed in real-time. Ultrasonic methods are non-invasive. When using ultrasonic methods for heating and imaging, both systems can be combined into one. Then, the effects disrupting the geometry of focusing can be minimized, because both, the therapeutic and imaging beams, are deformed in the same way, and only their relative position is an important parameter.

There are several ways for estimation of the temperature rise from the data available in standard medical US scanners. They are based on the phenomenon of a thermo-acoustic coupling, i.e. the relationship between some acoustic parameters and temperature.

The acoustic parameters used for the monitoring of temperature include

1. time shifts of echoes, caused by changes in tissue, thermal expansion, and the speed of sound
2. variations in acoustic attenuation
3. changes in the backscattered energy (CBE) of ultrasound
4. changes in parameters of statistics of the backscattered signal envelope.

The time shifts echoes result from thermal expansion of the heated tissue and, what's more important, from the temperature influence on sound velocity, which is described in [3]. Methods that utilize this phenomenon can be divided into time-domain and frequency-domain techniques. Time-domain algorithms [4-7] analyze return time delays of received echoes *via* the echo strain estimation. Frequency-domain methods [8,9] detect shifts in a spectral central frequency component of the received signal, which results from its time-compression due to sound velocity changes.

According to [3,10] the temperature also influences the acoustic attenuation. Therefore, methods for attenuation estimation such as the one presented in [11,12] can potentially be used for temperature imaging. Another temperature dependent parameter is the backscattered energy. It is frequently used by researchers to estimate the thermal field [13-19] due to the fact that it can be measured directly from a set of B-mode images as a mean grey level. Finally, the temperature changes can be assessed based on envelope statistics of the backscattered signal. The statistical approach is relatively new; thus, only a few papers are

available in this field. The published articles report on the usability of the Nakagami distribution for temperature estimation and evaluation of the ablated region [20-22].

The first of the above-mentioned methods - based on the analysis of time delays of echoes - was the basis for the development of an algorithm presented in this work. The algorithm processes the phase shifts of echoes received in successive moments of time, and calculates the relative changes in sound velocity as a result. In an initial approach, the proposed algorithm was verified qualitatively, which is described in our previous publication [23]. In the present paper, a more detailed analysis of the results obtained, using the modified algorithm, is presented and the research was concentrated on the first seconds of heating and the spatial extent of the heated area.

2. Theoretical basis

The sound velocity in tissue depends on the temperature [2]. Therefore, during the ultrasonic scanning of the heated tissue, changes in phase of the backscattered ultrasonic echoes are observed. Using the signal processing of the echoes, recorded from the scan lines, it is possible to estimate the spatio-temporal distribution of relative sound velocity changes, which can be next converted into the temperature field changes.

Let assume that φ_{1init} and φ_{2init} represent phases of the signal scattered in two axially adjacent sampling points 1 and 2:

$$\varphi_{1init} = 2\pi F_n \frac{2z}{c_0} \qquad \varphi_{2init} = 2\pi F_n \frac{2\left(z+\Delta z\right)}{c_0} \tag{1}$$

where z denotes the depth, k is the wave number for the nominal frequency $F_{n,}$ and the sound velocity c. Here Δz is the axial distance between two neighboring sampling points, while c_0 stands for the sound velocity before any thermal changes. When the heating probe is switched on, the sound velocity changes by Δc and formulas (1) are modified as follows:

$$\varphi_1 = 2\pi F_n \frac{2z}{c_0+\Delta c} \qquad \varphi_2 = 2\pi F_n \frac{2\left(z+\Delta z\right)}{c_0+\Delta c} \tag{2}$$

Let φ_1^* and φ_2^* represent the phase shifts at the considered locations resulting from tissue heating:

$$\varphi_1^* = \varphi_1 - \varphi_{1init} = 2\pi F_n 2z\left(\frac{1}{c_0+\Delta c} - \frac{1}{c_0}\right) \tag{3}$$

$$\varphi_2^* = \varphi_2 - \varphi_{2init} = 2\pi F_n 2\left(z+\Delta z\right)\left(\frac{1}{c_0+\Delta c} - \frac{1}{c_0}\right) \tag{4}$$

then, the difference between the phase shifts $\Delta\varphi$ can be described as:

$$\Delta\varphi = \varphi_2^* - \varphi_1^* = 2\pi F_n 2\Delta z \frac{-\Delta c}{\left(c_0+\Delta c\right)c_0} \tag{5}$$

Because the value of Δc is small compared to c_0, $c_0 + \Delta c \approx c_0$ the equation (4) can be rewritten as:

$$\Delta\varphi = 2\Delta z k_0 \frac{-\Delta c}{c_0} \qquad \text{and} \qquad \frac{\Delta c}{c_0} = \frac{-\Delta\varphi}{2\Delta z k_0} \tag{6}$$

gives the final formula for relative changes in the sound velocity.

The proposed algorithm is based on Equation (6). Values k_0 and Δz are known, while $\Delta\varphi$ can be derived from the received RF signal waveforms. RF scan-lines are filtered to remove both the high frequency noise, and low frequency interference due to HIFU. The phase of each signal is determined using a Hilbert transform, and calculating the argument of the resulting complex analytic signal.

The relative change of the sound velocity in the sample is calculated according to the following formula, being equivalent to the equation (6):

$$\frac{\Delta c}{c_0} = \frac{-\left(\varphi^*\left(x, z+\Delta z, n\right) - \varphi^*\left(x, z, n\right)\right)}{2\Delta z k} \tag{7}$$

where n is the number of imaging frame. Because the processing involves differentiation of the function φ^*, the high frequency components are amplified, and the results are noisy. Therefore, at a final step a spatial smoothing is applied to improve the readability of the obtained data.

3. Measurements

The measurement setup consisted of a HIFU system, a thermocouple system, the ultrasonic imaging system SonixTOUCH with a linear probe (L14-5/38), a water bath made of acrylic glass (PMMA), and filled with degassed distilled water with a controlled temperature, and a tested tissue sample placed in a cylindrical chamber and immersed in the water bath (Fig. 1).

Pork loin *in vitro* was used to prepare the tissue samples. Each sample was cut using a pipe cutter, degassed and inserted in a cylindrical chamber with an inner diameter of 40 mm and height of 40 mm.

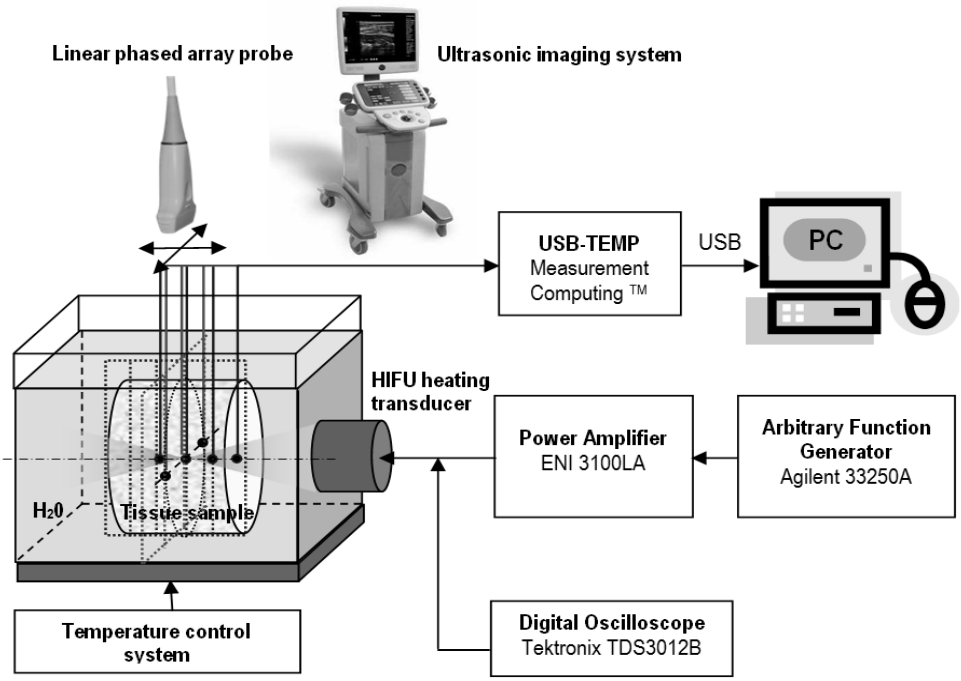

Fig. 1. Block-scheme of the experimental setup for invasive and non-invasive measurements of local thermal fields induced in soft tissues by pulsed high intensity focused ultrasound.

The HIFU system included a circular focused transducer with a diameter of 44.5 mm, 44.5 mm radius of curvature, and 2 MHz resonance frequency. The HIFU transducer was mounted in the wall of the water bath, coaxially with the tissue sample. The position of the focal plane of the HIFU beam was approximately in the center of the sample. The transducer was driven by 20-cycle tone bursts at a 2 MHz frequency (duty cycle - 20%, 10 μs bursts repeated every 50 μs). The amplitude of the excitation was adjusted so that the average emitted acoustic power measured with an ultrasound power meter (Ohmic Instruments UPM DT 1E, Easton, USA) was equal to 4 W. The tissue samples were subjected to heating for 15 minutes, which resulted in maximum temperature rise in focus from 20.4°C to 55.7°C. Then, the samples were cooled down.

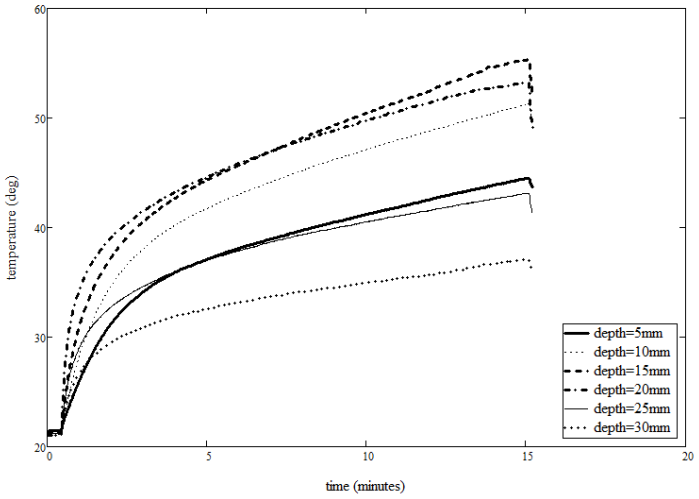

Fig. 2 Temperature rise in a pork loin *in vitro* during sonification by HIFU beam with average acoustic power of 4 W and measured along the acoustic beam axis using thermocouples located in the tissue sample at the depth of 5, 10, 15, 20, 25 and 30 mm from sample surface.

In a first approach, the temperatures were measured with thermocouples, as shown in Fig. 1. The thermocouple system included a set of thermocouples with a diameter of 0.2 mm, a temperature measurement device (Measurement Computing USB-TEMP, Norton, USA) and a PC with a software package (Measurement Computing TracerDAQ, Norton, USA) for visualization of the measurement data. The thermocouples were injected into the tissue sample using hypodermic needles with a diameter of 0.5 mm, fixed to the bath cover to ensure their precise positioning on the HIFU beam axis, in steps of 5 mm. The temperature rise detected by each thermocouple was recorded at 1 second steps by the USB-TEMP, transferred to the PC, and visualized with the TracerDAQ (see Fig.2). The obtained results were used to localize a position, and to measure the maximum temperature rise in the tissue sample.

Then, the tissue sample was replaced with the new one (prepared from the same piece of pork loin) and the SonixTOUCH system was used instead of the thermocouple system, as shown in Fig. 1. The sample chamber was designed so that the imaging probe could be coupled directly to the sample. The imaging plane was perpendicular to the heating beam axis, and located at the position of the maximum temperature rise. The sample was scanned with the SonixTOUCH system at intervals of 5 seconds. Similarly to the previous measurements, the STA technique (24) was applied, and 3 periods of a sine wave at a frequency of 8 MHz were transmitted. The collected raw RF data were reconstructed, and then processed with the proposed algorithm in the Matlab environment.

4. Results

The developed algorithm provides the ability to estimate the relative spatio-temporal changes in the velocity of sound in soft tissues. The results of the experiment, which included heating of the tissue sample *in vitro* using HIFU, were curves of velocity changes with temperature (Fig. 3), B-mode images presented in Fig. 4 and maps of the sound velocity changes shown in Fig. 5 and 6.

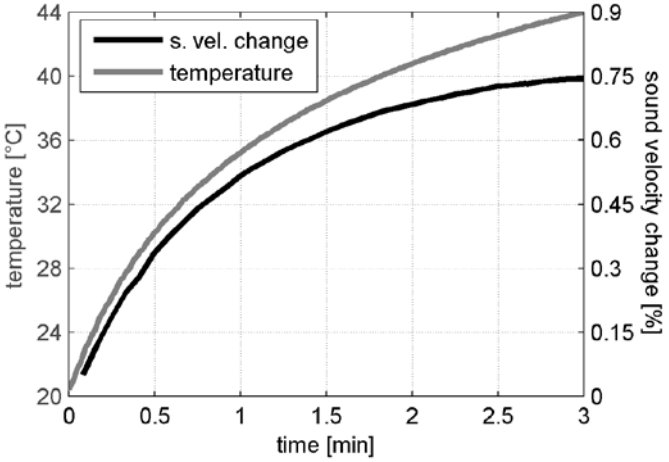

Fig. 3 Variation of sound velocity (algorithm) and temperature (thermocouple) in tissue determined in focus of HIFU beam, during the first 3 minutes of heating.

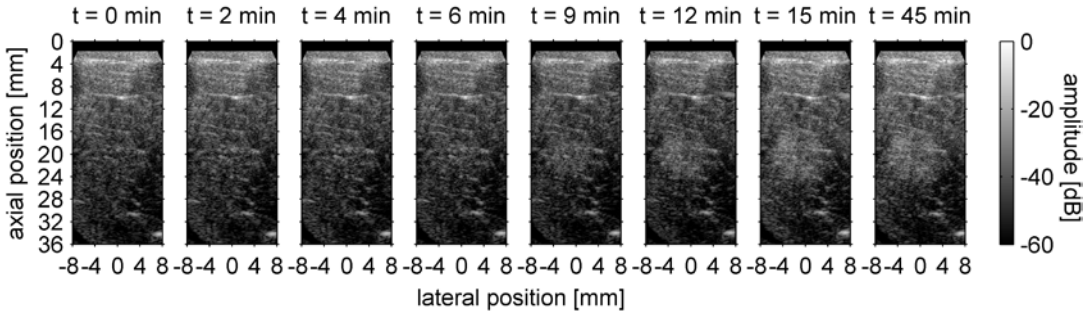

Fig. 4. B-mode images of the tested tissue structure at selected moments during the heating with HIFU. For $t \leq 9$ min the temperature is not sufficiently high to cause a visible tissue structure change. For $t > 9$ min, the temperature is high enough to cause irreversible tissue structure changes, which are visible in B-mode.

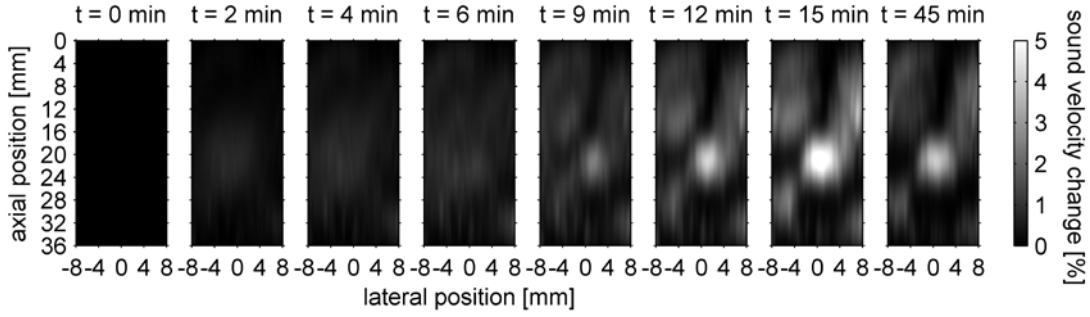

Fig. 5. Maps of the relative changes in the sound velocity in the tissue sample at selected moments during 15 min of heating with HIFU, and 30 min of cooling. The heated area is visible prior to the ablation stage of the experiment.

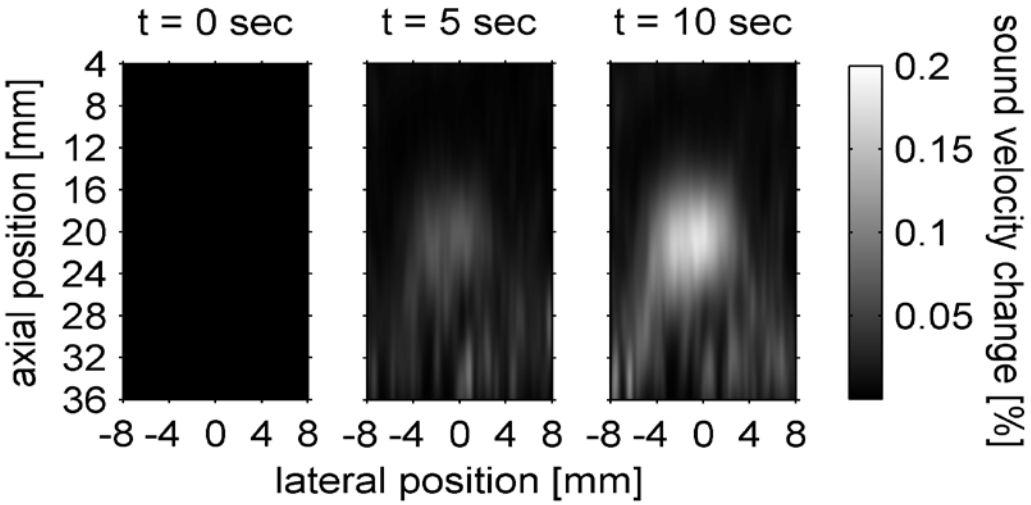

Fig. 6. Maps of the relative changes in the sound velocity in the tissue sample at fifth and tenth second of heating. The heated area is visible long before the ablation stage of the experiment.

To quantify the minimum contrast-to-noise ratio, required for visualizing and distinguishing between the heated tissue area, and unheated background, for both, the 2D sound velocity distributions and standard B-mode images, the contrast-to-noise ratio (CNR) was determined as:

$$CNR = \frac{S_t - S_b}{\sqrt{\frac{\sigma_t^2 + \sigma_b^2}{2}}}, \tag{8}$$

where S_t and S_b are mean values of signals (parameter c or B-mode image brightness) in the target region and background, respectively, while σ_t and σ_b denote the standard deviation of this measured quantity in the target and background (see Fig. 7)

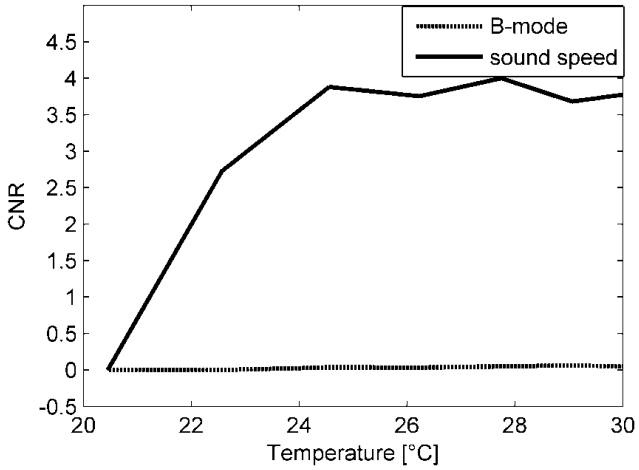

Fig. 7 Contrast-to-noise ratio as a function of temperature for both, the B-mode (dashed line) and sound speed distribution (continuous line) images of the heated region. First 30 seconds of heating.

The spatial extent of changes in the tissue velocity during heating was also determined. During 180sec. the temperature in focus increased by 23°C up to 43°C. Above this temperature, changes in the tissue structure are irreversible, and they are the main reason of velocity variation. In Fig.8, spatial distribution of the velocity changes along the vertical cross-section of the focal spot is presented. 7mm distance (see Fig.8, 900sec. of heating) corresponds to the velocity change of approximately 1.8% and temperature over 50 °C (see Fig.9, on right). After the measurements, the pork sample was cut along the acoustic beam direction, and the cross-section of the sample is presented in Fig. 9, on the left. The area corresponding to tissue necrosis is well visible. The extent of the necrosis in the beam focus equals around 7mm.

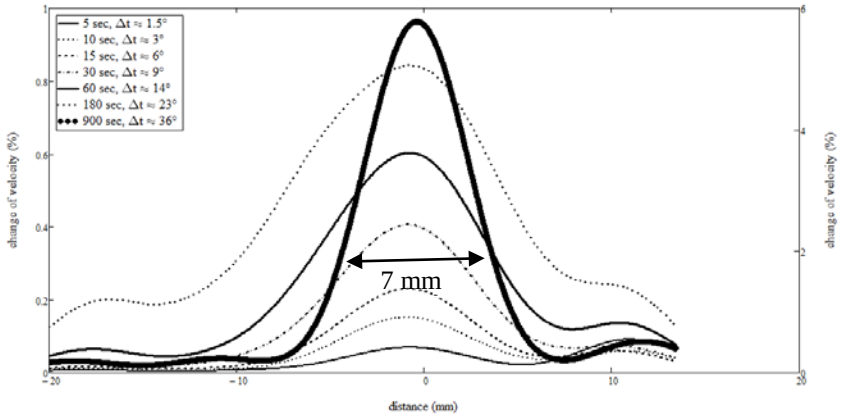

Fig. 8 Spatial distribution of the sound velocity variation due to heating. According to Figs.5 and 6, the vertical section is presented. Ultrasonic data was determined across the heating beam during 15 minutes of heating that resulted in a temperature increase in the focus up to 36°C, and sound velocity variation by 6%. Please note a separate scale for the 900sec. curve.

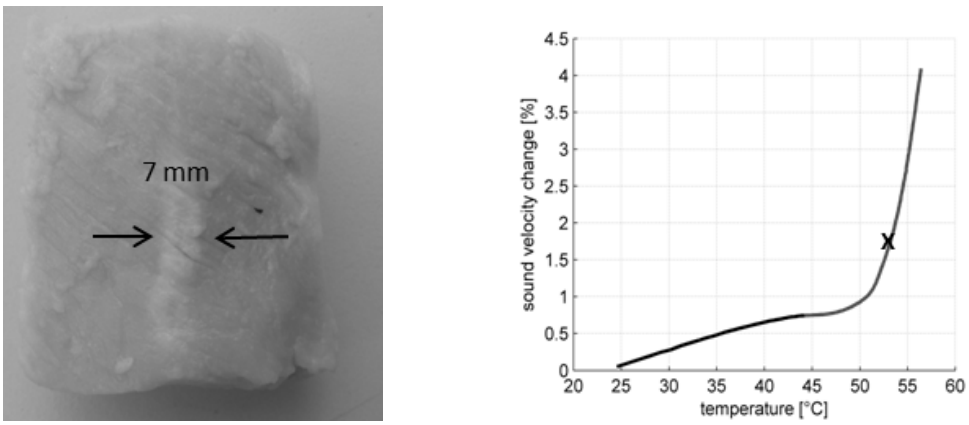

Fig. 9 Cross-section of the heated pork sample (left), and dependence of the sound velocity change in pork tissue in function of temperature (right).

5. Conclusions

The experiment, involving the heating of a tissue sample by HIFU, was performed to evaluate the proposed algorithm, using the data collected in conditions close to the in vivo measurements. The obtained results showed that the proposed method allows you to localize the position of the focal spot in the HIFU beam, before any irreversible thermal changes in tissue structure appear; which is impossible using only the standard B-mode images. Moreover, the maps of the sound velocity changes offer much higher contrast in the imaging

of the thermally damaged tissue regions (Fig.7). This, potentially, provides a better control over the process of tissue thermal ablation.

At the present state of study the heat diffusion from the HIFU focal spot makes it impossible to discuss the resolution of the implemented method. Regarding the heat diffusion, one has to be aware that the target applications of the developed algorithm for tissues *in vivo* additionally include perfusion, which can greatly intensify the problem. Thus, in our future work, we plan to increase the power of the heating beam. This will, potentially, quicken the experiment and, consequently, reduce the impact of the heat diffusion on the evaluation of the developed algorithm.

Acknowledgments

The financial support of the Ministry of Science and Higher Education of Poland and the National Science Centre – Poland (Projects 2011/01/B/ST7/06728; 2011/01/B/ST7/06735; 2011/03/B/ST7/03347) is gratefully acknowledged.

References

[1] Pavel S. Yarmolenko, Eui Jung Moon, Chelsea Landon, Ashley Manzoor, Daryl W. Hochman, Benjamin L. Viglianti, Mark W. Dewhirst, Thresholds for thermal damage to normal tissues: An update, Int J Hyperthermia.; 27(4): 320–343, 2011.

[2] Hynynen K, MRI-guided focused ultrasound treatments. Ultrasonics 50: 221-229, 2010

[3] Bamber JC, Hill CR Ultrasonic attenuation and propagation speed in mammalian tissues as a function of temperature. Ultrasound Med Biol 5: 149–157, 1979.

[4] Maass-Moreno R, Damianou CA Noninvasive temperature estimation in tissue via ultrasound echo-shifts. Part I. Analytical model. J Acoust Soc Am 100(4): 2514–2521, 1996.

[5] Maass-Moreno R, Damianou CA Noninvasive temperature estimation in tissue via ultrasound echo-shifts. Part II. In vitro study. J Acoust Soc Am 100(4): 2522–2530, 1996.

[6] Simon C, VanBaren P, Ebbini E Two-dimensional temperature estimation using diagnostic ultrasound. IEEE Trans Ultrason Ferroelectr Freq Control 45(4): 1088–1099, 1998.

[7] Miller NR, Bamber JC, Meaney PM Fundamental limitations of noninvasive temperature imaging by means of ultrasounds echo strain estimation. Ultrasound Med Biol 28(10): 1319–1333, 2002.

[8] Souchon R, Bouchoux G, Maciejko E, Lafon C, Cathignol D, et al. Monitoring the formation of thermal lesions with heat-induced echo-strain imaging: a feasibility study. Ultrasound Med Biol 31(2): 251–259, 2005.

[9] Ye G, Smith PP, Noble JA Model-based ultrasound temperature visualization during and following HIFU exposure. Ultrasound Med Biol 36(2): 234-249, 2010.

[10] Seip R, Ebbini ES Noninvasive estimation of tissue temperature response to heating fields using diagnostic ultrasound. IEEE Trans Biomed Eng 42: 828–839, 1995.

[11] Liu HL, Li ML, Shih TC, Huang SM, Lu IY, et al. Instantaneous frequency-based ultrasonic temperature estimation during focused ultrasound thermal therapy. Ultrasound Med Biol 35(10): 1647-1661, 2009.

[12] Straube WL, Arthur RM Theoretical estimation of the temperature dependence of backscattered ultrasonic power for noninvasive thermometry. Ultrasound Med Biol 20(9): 915–922, 1994.

[13] Arthur RM, Straube WL, Starman JD, Moros EG Noninvasive temperature estimation based on the energy of backscattered ultrasound. Med Phys 30(6): 1021–1029, 2003.
[14] Guiot C, Cavalli R, Gaglioti P, Danelon D, Musacchio C, et al. Temperature monitoring using ultrasound contrast agents: in vitro investigation on thermal stability. Ultrasonics 42: 927–930, 2004.
[15] Trobaugh JW, Arthur RM, Straube WL, Moros EG A simulation model for ultrasonic temperature imaging using change in backscattered energy. Ultrasound Med Biol 34(2): 289–298, 2008.
[16] Shishitani T, Matsuzawa R, Yoshizawa S Changes in backscatter of liver tissue due to thermal coagulation induced by focused ultrasound. J Acoust Soc Am 134(2): 1724-1730, 2013.
[17] Xia J, Li Q, Liu HL, Chen WS, Tsui PH An Approach for the Visualization of Temperature Distribution in Tissues According to Changes in Ultrasonic Backscattered Energy. Comput Math Methods Med, 2013.
[18] Teixeira CA, Alvarenga AV, Cortela G, von Krüger MA, Pereira WCA Feasibility of non-invasive temperature estimation by the assessment of the average gray-level content of B-mode images. Ultrasonics 54(6): 1692-1702, 2014.
[19] Chen BT, Shieh J, Huang CW, Chen WS, Chen ZR, et al. Ultrasound thermal mapping based on a hybrid method combining physical and statistical models. Ultrasound Med Biol 40(1): 115–129, 2014.
[20] Tsui PH, Shu YC, Chen WS, Liu HL, Hsiao IT, et al. Ultrasound temperature estimation based on probability variation of backscatter data. Med Phys 39(5): 2369-2385, 2012.
[21] Zhang S, Zhou F, Wan M, Wei M, Fu Q, et al. Feasibility of using Nakagami distribution in evaluating the formation of ultrasound-induced thermal lesions. J Acoust Soc Am 131(6): 4836-4844, 2012.
[22] Rangraz P, Behnam H, Tavakkoli J Nakagami imaging for detecting thermal lesions induced by high-intensity focused ultrasound in tissue. Proc Inst Mech Eng H 228(1): 19-26, 2014.
[23] Karwat P., Kujawska T., Lewin P.A., Secomski W., Gambin B., Litniewski J., Determining temperature distribution in tissue in the focal plane of the high (>100 W/cm2) intensity focused ultrasound beam using phase shift of ultrasound echoes, Ultrasonics, 65, pp.211-219, 2016.
[24] Jensen JA, Nikolov SI, Gammelmark KL, Pedersen MH Synthetic aperture ultrasound imaging. Ultrasonics 44: pp5–15, 2006.